PCCP

Urea hydration from dielectric relaxation spectroscopy: old findings confirmed, new insights gained

Journal:	*Physical Chemistry Chemical Physics*
Manuscript ID	CP-ART-12-2015-007604
Article Type:	Paper
Date Submitted by the Author:	09-Dec-2015
Complete List of Authors:	Agieienko, Vira; Kazan Federal University, Physical Chemistry Buchner, Richard; Universität Regensburg, Physikalische und Theoretische Chemie

Journal Name

ARTICLE

Urea hydration from dielectric relaxation spectroscopy: old findings confirmed, new insights gained

Vira Agieienko[a] and Richard Buchner[b]

Received 00th January 20xx,
Accepted 00th January 20xx

DOI: 10.1039/x0xx00000x

www.rsc.org/

We report results on urea hydration obtained by dielectric relaxation spectroscopy (DRS) in a broad range of concentrations and temperatures. In particular, the effective hydration number and dipole moment of urea have been determined. The observed changes with composition and temperature were found to be insignificant and mainly caused by the changing number density of urea. Similarly, solute reorientation scaled simply with viscosity. In contrast, we find that water reorientation undergoes substantial changes in the presence of urea, resulting in two water fractions. The first corresponds to water molecules strongly bound to urea. These solvent molecules follow the reorientational dynamics of the solute. The second fraction exhibits only a minor increase of its relaxation time (in comparison with pure water) which is not linked to solution viscosity. Its activation energy decreases significantly with urea concentration, indicating a marked decrease of the number of H-bonds among the H_2O molecules belonging to this fraction. Noncovalent interactions (NCI) analysis, capable to estimate the strength of the interactions within a cluster, shows that bound water molecules are most probably double-hydrogen bonded to urea via the oxygen atom of the carbonyl group and a *cis*-hydrogen atom. Due to the increased H-bond strength compared to the water dimer and the rigid position in the formed complex the reorientation of these bound H_2O molecules is strongly impeded.

Introduction

Aqueous urea solutions have been investigated in detail experimentally, using among other techniques IR[1-3] and Raman spectroscopy,[4-6] NMR,[7-9] dielectric relaxation spectroscopy (DRS),[10-16] optical Kerr effect,[6,17,18] THz spectroscopy,[19,20] neutron diffraction,[21-24] and X-ray scattering.[25] They were also the aim of many molecular dynamics (MD) simulations.[26-38] These and other studies focused on two important general aspects of aqueous solutions. The first issue concerns changes in the water structure within and beyond the hydration layer of the solute, whereas the second is related to changes in water dynamics.

However, despite such a plethora of experimental and theoretical investigations, there is still no consensus regarding the behaviour of water in the presence of urea as studies dealing with structural aspects yielded conflicting results. For instance, Åstrand[26] concluded from MD simulations that urea fits into the water network structure and even maintains the tetrahedral ordering of liquid water. This conclusion is in agreement with IR[1] and NMR investigations[8] and also the recent MD studies by Carr *et al.*[38] and by Stumpe and Grubmüller[36] who found that urea causes only minor structural perturbations of water. In contrast to that, also on the base of MD simulations, Idrissi and co-workers[34] claimed a marked distortion of the tetrahedral arrangement of water molecules upon urea addition.

By analyzing the lifetime of water molecules in the bulk and in the vicinity of the solute Kokubo *et al.*[35] showed that the H-bonds between water molecules are almost not affected by the presence of urea. Also, an earlier investigation using THz absorption spectroscopy found no indications of a long-range effect on the H-bond dynamics.[19] A similar conclusion was reached by Rezus and Bakker[3] from the analysis HDO orientational dynamics in aqueous urea solutions. This interpretation, however, was not supported by an analysis of the Raman spectral density[6] that indicated a significantly disrupted water-water H-bond structure at $c > 1$ M. Reduced water density and enhanced solvent mobility were also evidenced in MD simulations of Kallies.[29] In agreement with the latter, a Monte-Carlo study of {urea+water} mixtures[27] suggested that urea breaks the water-water network.

Although the behaviour of water molecules beyond the first solvation shell of urea is still disputed, their substantial retardation in the direct proximity of the solute is confirmed by various spectroscopic techniques. Depending on temperature, solute concentration and method of investigation the number of water molecules strongly bound to urea was found to be within the range 0.5-4.3.[3,5,11,12,15,16,19] However, several MD studies[26,29,39,40] reported significantly larger coordination numbers of urea as well as higher numbers of water molecules H-bonded to its hydrophilic groups. Based on the results obtained with different spectroscopic

[a] *Department of Physical Chemistry, Kazan Federal University, Kremlevskaya str. 18, 420008 Kazan, Russia*
[b] *Institut für Physikalische und Theoretische Chemie, Universität Regensburg, D-93040 Regensburg, Deutschland*

† Electronic Supplementary Information (ESI) available: [Tables with data for density and viscosity, and with relaxation parameters describing the dielectric spectra; auxiliary figures]. See DOI: 10.1039/x0xx00000x

techniques,[3,15,19] several authors proposed that the water molecules forming one H-bond with a urea molecule are only weakly bound and show dynamics similar to water in bulk. In contrast to that, water molecules forming two hydrogen bonds with urea are strongly immobilized. This view gains support from the MD simulations of Åstrand *et al.*,[26] who reported that the orientational correlation functions of the out-of-plane (reorientation of the *y*-axis, Fig. 1) and in-plane (*x*-axis, Fig. 1) motions of urea decay much faster than the correlation function of the dipole moment vector (*z*-axis, Fig. 1), indicating an anisotropic hydration structure. Idrissi and co-workers[41] studied {urea+water} systems using molecular dynamics simulations and optical Kerr effect. Analyzing the power spectra of the linear velocity auto-correlation functions of urea, they concluded that this molecule experiences H-bonding preferentially in the dipole-moment and out-of-plane directions. Additionally, the observed anisotropic reorientation of urea around its principal axes[17] was interpreted as a consequence of the highly directional H-bonding interaction. A more recent MD study[29] revealed pronounced structuring of the water molecules around the oxygen and *trans*-hydrogen atoms of urea. It was found that the water molecules coordinating to these groups are preferentially located in the plane of the solute and show parallel alignment of their dipole vectors with that of urea. In agreement with the latter, Raman difference spectra of dilute solutions did not indicate specific interactions of water molecules in the direction of the CN bond of urea.[4]

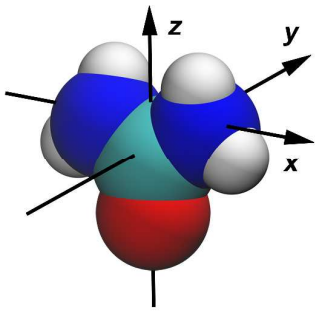

Fig. 1. A urea molecule with its principal axes of inertia.

Besides hydration effects, the possible self-aggregation of urea molecules with increasing solute concentration has been also considered as an explanation for the behaviour of aqueous urea solutions. In a 2D IR study[2] the peaks obtained in the concentration range of 0.5-2.0 M urea were assigned to cyclic and linear dimers. At higher concentrations, crosspeaks corresponding to larger oligomers were found. According to MD simulations of Soper *et al.*[30] only 11% of the dissolved urea molecules are present as monomers in a ~ 13.5 M solution, whereas the rest forms dimers or higher aggregates. The idea of urea dimerization at $c > 0.83$ M is also supported by a Monte-Carlo study[27] and according to the simulations of Stumpe and Grubmüller[36] ~20 % of the urea molecules are aggregated in a 9 M solution. On the other hand, Funkner *et al.*[19] found no urea self-aggregation up to 4 M with far-infrared spectroscopy. The results of quantum chemical calculations[42,43] showed that cyclic urea dimers tend to be separated into solvated monomers in aqueous solution. Also DRS[10] and Raman[5] studies found no evidence of urea self-association.

In this work, we apply DRS to investigate the dynamics of aqueous urea solutions over a wide concentration range at 25 °C. This technique probes all solution dynamics associated with a change of the macroscopic dipole moment of the sample in terms of the complex permittivity

$$\hat{\varepsilon}(\nu) = \varepsilon'(\nu) - i\varepsilon''(\nu)\,, \qquad (1)$$

where $\varepsilon'(\nu)$ is the relative permittivity and $\varepsilon''(\nu)$ the dielectric loss at frequency ν.[44,45] This technique is able to resolve the contributions of the various dipolar species present in solution provided they differ in reorientational dynamics, *i.e.* exhibit different relaxation times. For selected solutions, DRS measurements were also performed at (5 and 45) °C to obtain activation energies and thus get deeper insight into the mechanism of both solute and solvent reorientation. We also show the results of a noncovalent interactions (NCIs) analysis of selected urea hydrates. This recently developed technique, based on the analysis of wave functions, is a powerful tool for estimating the strength and localization of specific interactions within a complex.

Experimental section

Solutions were prepared by weight on an analytical balance without buoyancy corrections using urea (Sigma Aldrich, ≥ 99.5%) and Millipore Milli-Q water. The samples covered solute molalities (moles urea per kg water) of $m \le 17.994$ mol kg^{-1}. The secondary calibration standards for the DRS experiments, propylene carbonate, N,N-dimethylacetamide and formamide (all Sigma Aldrich), were stored over freshly activated molecular sieves (4 Å) for several days before use.

To cover the broad frequency range of the present DRS experiments ($0.05 \le \nu$ / GHz ≤ 89), several set-ups were combined. For $0.05 \le \nu$ / GHz ≤ 50 dielectric spectra were measured with a frequency-domain reflectometer based on Agilent 85070E-20 and 85070E-50 dielectric probes connected to an Agilent E8364B vector network analyzer (VNA).[46] Air, mercury and water were used as primary calibration standards. Calibration errors were corrected with a Padé approximation using liquids with known dielectric properties as secondary standards.[47] Depending on urea concentration two different sets of secondary standards were appropriate. At $m \le 4.0$ mol kg^{-1}, propylene carbonate and N,N-dimethyl-acetamide were used, whereas at higher concentrations better results were obtained with propylene carbonate and formamide. The choice of the secondary standards was based on the analysis of the reduced error function, χ_r^2,[48] of the fit of the spectrum and a crosscheck with data recorded with a variable-pathlength 27-39 GHz waveguide transmission cell hooked to the VNA. The latter does not require calibration. The data from the two reflection probeheads were

concatenated at ~ 2 GHz and combined with those from a waveguide interferometer operating at $60 \le \nu$ / GHz ≤ 89.[49] Due to the small residual conductivity of the samples raw spectra were corrected for the DC conductivity determined from the low-frequency limit of the dielectric loss and data at ν < 100 MHz discarded. The obtained spectra of $\varepsilon'(\nu)$ (A) and $\varepsilon''(\nu)$ (B) are shown in Fig. 2 and in Fig. S1 of the Electronic Supporting Information (ESI).†

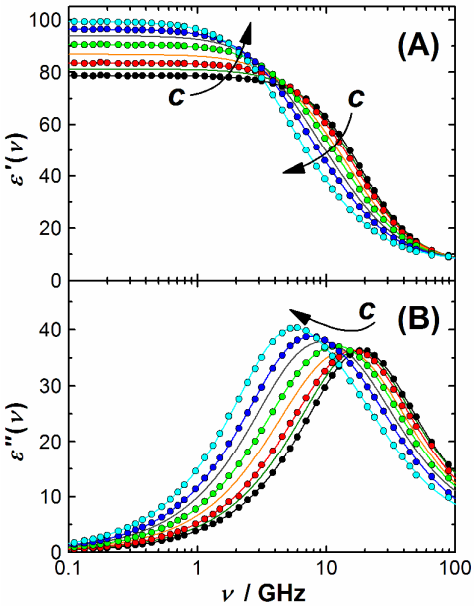

Fig. 2. Spectra of (A) relative permittivity, $\varepsilon'(\nu)$, and (B) dielectric loss, $\varepsilon''(\nu)$, of aqueous solutions of urea at 25 °C and solute molalities $m \le 17.994$ mol kg^{-1}. Symbols represent the experimental data, lines the fit with the 3D model. The arrows indicate the direction of increasing urea concentration.

Densities, d, required for converting from molal, m, to molar concentrations, c [in M = mol L^{-1}], were measured with an Anton Paar DMA 5000 M vibrating tube densimeter. Viscosity was determined with an Anton Paar AMVn rolling ball viscometer using a 1.6 mm capillary calibrated with degassed Millipore Milli-Q water. The data are summarized in Table S1.† Most measurements of $\hat{\varepsilon}(\nu)$, d and η were performed at 25 °C. Additionally, the samples with (1.999, 6.001, and 11.995) mol kg^{-1} urea were investigated at (5 and 45) °C. The temperature uncertainty was (± 0.05, ± 0.005 and ± 0.01) °C for DRS, density and viscosity measurements, respectively.

For a quantitative analysis of the dielectric spectra these were fitted to relaxation models assumed to be sums of n independent modes, j,

$$\hat{\varepsilon}(\nu) = \varepsilon_\infty + \sum_{j=1}^{n} \frac{S_j}{[1+(i2\pi\nu\tau_j)^{1-\alpha_j}]^{\beta_j}} . \qquad (2)$$

The latter were represented by the Havriliak-Negami (HN) equation (shape parameters $0 \le \alpha_j < 1$ and $0 < \beta_j \le 1$), or its simplified variants, the Cole-Davidson (CD, $\alpha_j = 0$), Cole-Cole (CC, $\beta_j = 1$), and Debye (D, $\alpha_j = 0$, $\beta_j = 1$) equations, with amplitude S_j and relaxation time τ_j.[44] Ideally, the high-frequency permittivity, ε_∞, only comprises intra-molecular contributions but here it is a fitting parameter encompassing librational motions in the far-infrared region. The static permittivity of the sample is given by the sum of all individual contributions to the spectrum, *i.e.* $\varepsilon_s = \varepsilon_\infty + \sum_{j=1}^{n} S_j$.

Results

The relaxation model for {urea+water} mixtures. A literature search revealed several publications dealing with the dielectric relaxation of {urea+water} mixtures.[10-16] The earliest reported study[10] was just done at three frequencies but nevertheless assumed separate relaxations for water and urea. Pottel *et al.*[11] measured the complex permittivity of 1.0 and 2.0 M urea solutions between 0.3 and 38 GHz. The data were fitted to three D relaxations attributed to the reorientation of 'free' water, hydration water and urea itself. During the data processing the 'free' water relaxation time was assumed to be the same as in pure water. Since the relaxation times of hydration water and urea obtained in this study were very close to each other (~ 17 and ~ 19 ps, respectively) the reliability of this spectral decomposition can be disputed.[50] Indeed, in a later work with participation of the same authors,[12] studying 1.0 and 2.0 M solutions in the frequency range between 1 MHz and 40 GHz, the obtained spectra were represented as the sum of a CC process for water and a D mode for urea. To separate both contributions the solute amplitude was fixed together with the static permittivity of the solutions. Hayashi *et al.*[15,16] fitted their 0.2-40 GHz dielectric spectra of the {urea+water} system, covering $0.5 \le c$ / M ≤ 9.0, with two D relaxations attributed to bulk-water clusters and urea-water co-clusters. At c < 6.0 M a stable fit was obtained by freezing the relaxation time of the first to the pure-water value, 8.27 ps, and assuming 21.3 ps for the urea mode. However, this procedure was found to be inappropriate for higher urea concentrations. Here, freely floating relaxation times for both modes were more satisfactory and yielded water relaxation times < 8.27 ps. On the other hand, Saito *et al.*,[14] measuring dielectric spectra from 0.2 to 20 GHz at urea mole fractions of 0.025, 0.05, 0.075 and 0.1, used a single D relaxation assigned to bulk water whereas Bateman *et al.*[13] concluded that their 0.01-70 GHz spectra for urea mass fractions of 0.334, 0.359, and 0.399 could be fairly well reproduced by either two D or one CC relaxations, albeit without a clear concentration dependence of the relaxation times obtained with the 2D model. Data from terahertz time-domain spectroscopy of 1-10 M solutions covering 0.3-2.0 THz[20] were described by a superposition of three D modes. Since the urea mode was far outside the covered frequency range its relaxation time was fixed to the values reported in Ref. 15. This yielded ~ 9 ps for the intermediate and ~ 0.2 ps for the high-frequency mode, similar to data for pure water.[51] A 3D model was also used by Hunger *et al.*[52] for fitting their spectra covering the range $0.1 \ge \nu$ / GHz ≥ 1600. The high-frequency mode, centered at $\nu \approx 0.5$ THz, was assigned to a fast water relaxation, the main dipolar relaxation of water was

found to be at 13-20 GHz and that of urea at 5-8 GHz, depending on urea concentration. For this analysis the amplitude of the water relaxations was fixed to the value expected from the analytical solvent concentration, assuming the effective dipole moment to be equal to that of neat water.

According to this overview there is broad consensus on the existence of two distinct but not well separated relaxations for urea and water in the gigahertz region. Additionally, there are indications for a small-amplitude terahertz mode due to fast water. However, all previous studies made assumptions on the relaxation times or amplitudes of some of the resolved modes, introducing thus some bias in the discussion. To gain somewhat more objective insights into the number and character of the possible modes contributing to the present dielectric spectra, their relaxation time probability distribution function, $P(\tau)$, was determined with Zasetzky's method.[50] The results are shown in Fig. 3 and clearly indicate that the present $\hat{\varepsilon}(\nu)$ can be resolved into three modes. The fastest relaxation, of low intensity (cyan columns), is characterized by relaxation times scattering around 0.3-1.8 ps, corresponding to loss-peak frequencies of ~ 90-500 GHz just outside the experimental frequency range (Fig. 4). The other two processes, with $\tau \approx 8.5$ ps (~ 15-18 GHz, green columns) and $\tau \approx 20$-34 ps (~ 5-9 GHz, red columns) have significantly larger $P(\tau)$ values, which decrease for the intermediate-frequency relaxation and increase for the lower-frequency mode (Fig. 3). Both modes exhibit a smooth low-frequency shift of their peak frequencies with increasing solute concentration (Fig. 4B).

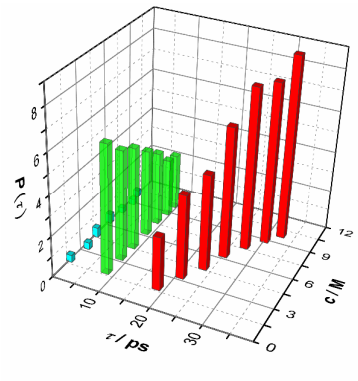

Fig. 3. Relaxation-time distribution function, $P(\tau)$, of aqueous urea solutions ($c \geq 2$ M) at 25 °C obtained with the fitting procedure of Zasetsky.[50] Cyan, green and red columns represent the relaxations of fast water, bulk-like water and urea, respectively.

The outcome of the Zasetsky analysis was confirmed by fits of the experimental spectra with relaxation models based on eqn (2), where all reasonable combinations of band-shape functions up to $n = 4$ were tested. For all concentrations and at all temperatures the sum of three Debye relaxations, hereafter called the 3D model (Fig. 4A), performed best, yielding the smallest χ_r^2 values and parameters smoothly varying with concentration (Figs. 4B and S2†). Note that for the measurements at 45 °C the shortest relaxation time had to be

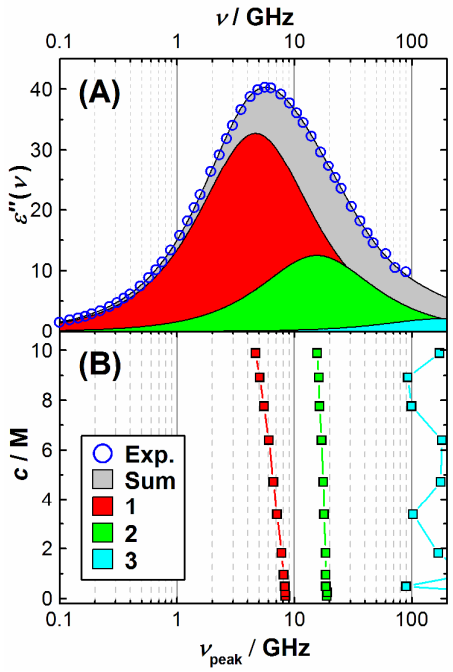

Fig. 4. (A) Dielectric loss spectrum, $\varepsilon''(\nu)$ (○), of 10 M aqueous urea at 25 °C and its fit with the 3D model (line). The shaded areas in panel (A) show the contributions of the resolved modes with their peak positions as a function of concentration given in panel (B).

fixed at $\tau_3 = 0.17$ ps because of the considerable high-frequency shift of all modes at that temperature. Also, for urea molalities of $m < 1$ mol kg^{-1} of the 25 °C series the relaxation time of the lower-frequency mode, $\tau_1(m)$, was fixed to values linearly extrapolated from the data at higher concentrations to minimize the scatter of the corresponding small amplitudes, $S_1(m)$ (Fig. S2†). The thus obtained fit parameters are given in Table S2.†

With increasing urea concentration, the amplitude of the slowest relaxation, S_1, which is not present for pure water,[51] quickly rises, yielding ~ 65.5 units at 10 M (Fig. S2†). This allows unambiguous attribution of this mode to the solute, in line with previous DRS studies.[11-16,52] However, as will be shown below, this relaxation is not solely due to the reorientation of urea molecules. From the concentration dependence of amplitude, S_2 (Fig. S2†), and relaxation time, τ_2 (Fig. 4B), the intermediate-frequency mode can be clearly assigned to the cooperative (structural, α-) relaxation of rather unperturbed water. The parameters found for the small high-frequency contribution, S_3 and τ_3, are comparable with the fast mode observed for pure water.[51] This contribution is most likely associated with the fast hydrogen-bond switch occurring in the jump-relaxation mechanism proposed for water by Laage *et al,*[53] which should also apply to {urea+water} mixtures. Note that the scatter of the present values for S_3 and τ_3 is not physical but reflects lacking terahertz data.

It should be noted here that in contrast to previous DRS studies of {urea+water} mixtures no assumptions were required to unequivocally separate solute and solvent contributions. In particular, it was not necessary to fix τ_2 to the value of pure water or S_2 to the value predicted by the analytical water concentration. As shown below, this has considerable implications for the interpretation of the data.

Water Relaxation

The issue most debated in literature regarding {urea+water} mixtures is how water molecules are affected by the presence of urea with regards to both structure and dynamics. Pottel and co-workers[11] inferred from their dielectric data that the number of water molecules strongly bound to urea is within the range 2.6-4.3. In a more recent paper with participation of the same authors[12] a hydration number of 2-3 was found. Unfortunately, it is not fully clear how these numbers were obtained. Also with DRS, a hydration number of two was obtained by Hayashi *et al.*[15,16], whereas Bateman *et al.*[13] found no evidence for a hydration shell around urea differing in dynamics from bulk water. Also Hunger *et al.*[52] assume negligible hydration. The time-resolved infrared experiments of Rezus and Bakker[3] yielded a single H_2O molecule per urea with significantly slowed-down dynamics compared to pure water, in line with Raman results.[5] From terahertz absorption spectra[19] it was deduced that the average number of water molecules bound to urea ranges from 0.5 at 9 °C to 1.1 at 36 °C and the authors argue that these H_2O molecules form two H-bonds with urea. Such kind of water binding was also suggested by Refs. 3 and 16.

On the other hand, also significantly larger hydration numbers have been reported for urea. An NMR study[9] yielded 6.68 ± 0.24,[54] whereas a value of 5.0 ± 0.5 was reported from IR-spectroscopic investigations.[55] These values are comparable to the coordination number of urea, $CN \approx 7$, deduced from scattering experiments.[56] Based on compressibility data, Avanas'ev[57] even reported hydration numbers between 13.37 and 6.55, decreasing with urea concentration. However, note that another compressibility study[58] only yielded 2.75. It should be kept in mind here that in contrast to *CN*, which is the generally well-defined number of next neighbours, experimental hydration numbers strongly depend on the method used for their determination.

Using a somewhat different approach[59] compared to Refs. 10-16, we found[45,60-62] for relaxation amplitudes, S_j, of modes, j, arising from the reorientation of permanent dipoles (gas-phase moment μ_j) that the concentration, c_j, of the dipolar species can be suitably obtained by the equation

$$\frac{\varepsilon_s + A_j(1-\varepsilon_s)}{\varepsilon_s} = \frac{N_A c_j}{3k_B T \varepsilon_0}\left(\mu_{j,\mathrm{eff}}\right)^2 , \qquad (3)$$

where N_A and k_B are the Avogadro and Boltzmann constants, T is the thermodynamic temperature, ε_0 is the vacuum permittivity, and A_j is the cavity-field factor.[59] The effective dipole moment, $\mu_{j,\mathrm{eff}} = g_j^{1/2} \times \mu_{j,\mathrm{ap}}$, of species j consists of its apparent dipole moment, $\mu_{j,\mathrm{ap}} = \mu_j / (1 - f_j \alpha_j)$, with α_j being the polarizability and f_j the corresponding reaction-field factor, and g_j as the equivalent to the Kirkwood correlation factor indicating orientational correlations of j-dipoles for $g_j \neq 1$.

For the evaluation of solvent amplitudes it is convenient to normalise eqn (3) to the pure solvent[63] and for water $A_j = 1/3$. Also, the fast (S_3, τ_3) and cooperative (S_2, τ_2) water modes do not represent different species but are characteristic steps in the time evolution of bulk-water dynamics.[53,63] Accordingly, their amplitudes have to be combined to yield the bulk-water amplitude

$$S_b(c) = S_2(c) + S_3(c) + \varepsilon_\infty(c) - \varepsilon_\infty(0) , \qquad (4)$$

(Fig. S2†). With the help of the high-frequency permittivity of pure water determined in the terahertz range, $\varepsilon_\infty(0) = 3.52$,[62] eqn (4) also accounts for the somewhat too large $\varepsilon_\infty(c)$ (and thus too small $S_3(c)$) values of the present spectra that arise from their limitation to $\nu \leq 89$ GHz.

Insertion of $S_b(c)$ into eqn (3) then yields the concentration of DRS-detected bulk-like water, c_b, which can be compared with the analytical solvent concentration, c_w. Fig. S3† shows that an increasing fraction, $f_b = c_b / c_w$, of the water present in {urea+water} mixtures does not contribute to S_b, reaching ~ 27% close to the saturation limit. The corresponding total hydration number of urea

$$Z_t = (c_w - c_b)/c , \qquad (5)$$

decreases linearly from 1.85 at infinite dilution to 0.83 at 10 M urea (Fig. 5).

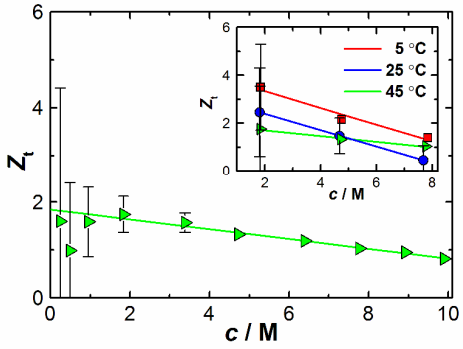

Fig. 5. Total hydration number of urea as a function of solute concentration at 25 °C. Symbols indicate the data obtained from DRS, line represents the result of a linear fit. The inset shows hydration numbers found for the three samples studied at (5, 25, and 45) °C.

The magnitude of Z_t is comparable to hydration numbers previously reported by some of the DRS studies,[12,16] by terahertz absorption[19] and time-resolved IR spectroscopy[3] but differs somewhat from urea hydration numbers derived from compressibility data[58] (2.75) and in particular from those of an NMR study[9] (6.68 ± 0.24)[54] and the coordination number from scattering experiments.[56] This clearly indicates that only some of the *CN* hydrating H_2O molecules are affected in their reorientational dynamics.

The most likely reason for the slight decrease of Z_t, which only becomes really detectable at c > 2 M, is solute crowding and the resulting hydration-shell overlap.[36, 64] Whilst for given c the Z_t values at 25 and 45 °C do not differ within error limits, the data for 5 °C appear to be systematically larger (Fig. 5, inset). This possibly suggests somewhat stronger hydration at low temperature, which is at variance to Ref. 19.

In contrast to aqueous solutions of tetramethylurea[65] or trimethylamine-*N*-oxide[60] no relaxation of 'slow' (moderately bound, retarded[53]) water could be resolved with the present spectra. This indicates that either the dynamics of the Z_t H_2O dipoles interacting with a urea molecule is practically frozen (implying the existence of long-lived hydrates) or that these solvent dipoles are retarded to such extent that their contribution coincides with the solute mode, i.e. that they are slaved to solute dynamics.

Urea Relaxation

By assuming that all urea molecules contribute to S_1, their effective dipole moment, μ_{eff}, was calculated with eqn (3) (Fig. 6). Within error limits, μ_{eff} decreases from (10.0 ± 0.1) D at $c \rightarrow 0$ to 8.8 D at c = 10 M. This result is in agreement with the data of Grant *et al.*[10] who reported for 20 °C μ_{eff} values for urea ranging from 10.2 D at 1.0 M to 8.4 D at 9.0 M. The present values are also in broad accordance with an earlier DRS study of 1.0 and 2.0 M aqueous urea solutions yielding 8.2 D,[12] as well as with μ_{eff} = (8.2 ± 1.0) D given by Hunger[52] for the concentration range $1.0 \le c / M \le 4.0$. Within experimental error the temperature dependence of μ_{eff} is negligible (Fig. 6, inset). In line with the data for Z_t (Fig. 5, inset) the slightly larger values for 5 °C may hint at stronger hydration for this temperature.

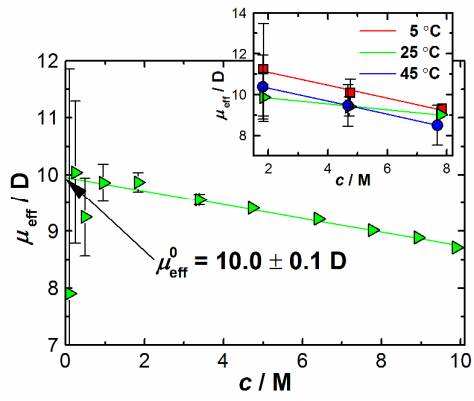

Fig. 6. Effective dipole moment, μ_{eff}, of urea in water as a function of concentration at 25 °C. The inset shows the effective dipole moment at different temperatures.

It must be noted that the value at infinite dilution, μ_{eff} = (10.0 ± 0.1) D, is significantly larger than the gas-phase dipole moment of urea, which was found to be (3.83 ± 0.04) D.[66] It is also inconsistent with the value of μ = 5.52 D obtained with quantum chemical calculations for a single urea molecule embedded in a water continuum.

One possible reason for such a big difference is binding of water molecules by urea (U) with a more-or-less parallel alignment of the molecular moments in the resulting complex. As shown above, approximately 1-2 water dipoles are indeed effectively immobilized by urea (Fig. 5). Analogous to tetramethylurea[65] and trimethylamine-*N*-oxide[60] it can be reasonably assumed that this bound water moves with the solute. Hence, the large values of μ_{eff} (Fig. 6) might result from the reorientation of stiff long lived $U{\cdot}H_2O$ and/or $U{\cdot}2H_2O$ complexes rather than isolated urea molecules. Alternatively, the dynamics of urea and their Z_t hydrating H_2O dipoles might be coupled, with the reorientation of both occurring on the timescale of τ_1.

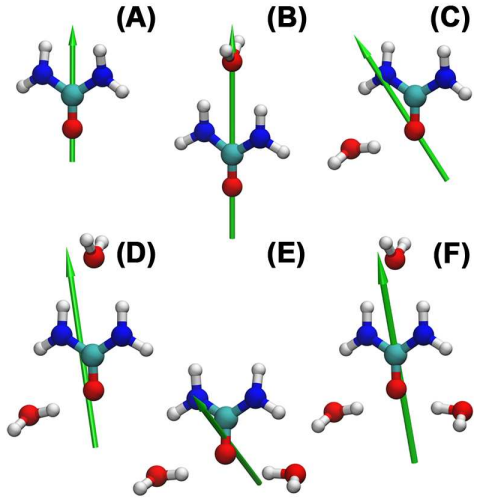

Fig. 7. Geometries of urea (A), $U{\cdot}H_2O$ (B, C), $U{\cdot}2H_2O$ (D, E) and $U{\cdot}3H_2O$ (F) complexes obtained at the B3LYP / 6-311++G(d,p) level of theory in a water continuum (ε = 78). The arrows indicate the dipole direction.

Table 1. Formation energies, ΔE, and dipole moments, μ, of urea (A, μ only), $U{\cdot}H_2O$ (B, C), $U{\cdot}2H_2O$ (D, E) and $U{\cdot}3H_2O$ (F) complexes in a vacuum and a water continuum (ε = 78) obtained at the B3LYP / 6-311++G(d,p) level of theory.

Structure	ΔE / kJ mol^{-1}	μ / D	ΔE / kJ mol^{-1}	μ / D
	vacuum		water	
Urea (A)		3.88		5.52
$U{\cdot}H_2O$ (B)	– 26.64	7.13	– 18.30	8.87
$U{\cdot}H_2O$ (C)	– 40.26	3.39	– 21.01	6.00
$U{\cdot}2H_2O$ (D)	– 69.01	6.62	– 41.04	9.19
$U{\cdot}2H_2O$ (E)	– 79.16	2.97	– 41.68	5.98
$U{\cdot}3H_2O$ (F)	– 109.87	5.84	– 62.52	9.19

In order to check the possible existence of aggregates, we performed quantum chemical calculations of U and various $U{\cdot}H_2O$, $U{\cdot}2H_2O$ and $U{\cdot}3H_2O$ complexes at the B3LYP/6-

311++G(d,p) level of theory both in a vacuum and a medium of water using the Gaussian 03 package.[67] Implicit solvent medium effects on the ground-state geometry were taken into account by the self-consistent reaction field method (SCRF) via the self-consistent isodensity polarizable continuum model (PCM)[68] implemented in the software. The most stable geometries of the complexes embedded in a continuum of water are shown in Fig. 7. Their formation energies and the dipole moment values are listed in Table 1.

Two stable $U{\cdot}H_2O$ structures have been found. For both the water molecule forms two hydrogen bonds to urea, either via the *trans*-hydrogen atoms (structure B) or via the carbonyl oxygen and a *cis*-hydrogen (structure C). In vacuo, the formation energies of structures B and C differ by ~ 14 kJ mol^{-1}, whereas embedded in the solvent continuum this difference is within the energy of thermal motion. In aqueous medium the dipole moments of these structures, μ(B) = 8.87 D, μ(C) = 6.00 D, are larger than that of an isolated urea molecule, μ(U) = 5.52 D. Also two energetically favorable $U{\cdot}2H_2O$ hydrates were found (structures D and E of Fig. 7; Table 1). In both cases, each of the two involved H_2O molecules forms two hydrogen bonds with urea. The dipole moments calculated for the water medium amount to μ(D) = 9.19 and μ(E) = 5.98 D. According to their energies of formation both are equally likely to occur in solution. Although not compatible with the obtained hydration numbers, $Z_t \leq 2$ (Fig. 5), calculations were also performed for a $U{\cdot}3H_2O$ complex, yielding a combination of structures B and E as the most stable species with a dipole moment of 9.2 D in water.

Although numerical agreement between experimental μ_{eff} values and dipole moments from cluster calculations should not be expected it appears that the assumption of $U{\cdot}H_2O$ and/or $U{\cdot}2H_2O$ (and $U{\cdot}3H_2O$) complexes is not sufficient to explain the rather high value of μ_{eff} = (10.0 ± 0.1) D at $c \rightarrow 0$ as structures B and C respectively D and E should be simultaneously present. This may hint at orientational correlations of the hydrated urea dipoles, as suggested by simulations of Stumpe and Grubmüller.[36] Unfortunately, this cannot be explored further with the present means.

Relaxation times. The comparison of relaxation times from different experimental techniques allows inference on the reorientation mechanism. Within the Debye model of rotational diffusion single-particle relaxation times, $\tau^{(n)}$, of rank *n* are interrelated by

$$\tau^{(n)} = \frac{2}{n(n+1)} \times \tau^{(1)}, \qquad (6)$$

where *n* is determined by the type of experiment. For dielectric and infrared (IR) spectroscopy *n* = 1, whereas for NMR, time-resolved IR, Raman or OKE spectroscopy *n* = 2. As the relaxation time probed by dielectric spectroscopy, τ_j, is a collective property it needs to be converted to the corresponding rotational correlation time, $\tau^{(1)}_{DRS,j}$, with the Powles-Glarum equation.[69, 70] For urea relaxation this takes the form

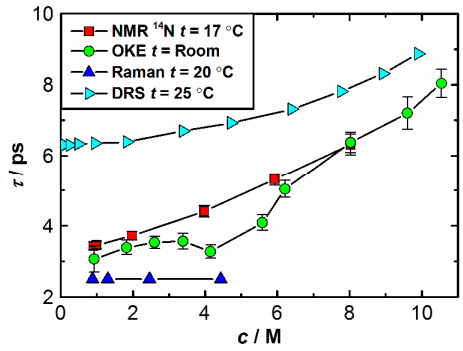

Fig. 8. Second order (*n* = 2) rotational correlation times obtained with NMR,[71] OKE,[17] and Raman[5] spectroscopy and corresponding DRS data, $\tau^{(1)}_{DRS,1}/3$, as a function of urea concentration.

$$\tau^{(1)}_{DRS,1} = \frac{2\varepsilon_s + \varepsilon_1}{3\varepsilon_s} \times \tau_1, \qquad (7)$$

where $\varepsilon_1 = \varepsilon_s - S_1$ and represents the low-frequency plateau of the water contribution to $\varepsilon'(\nu)$.

Complying with eqn (6), Fig. 8 compares the present values of $\tau^{(1)}_{DRS,1}/3$ with second-order rotational correlation times, $\tau^{(2)}$, from ^{14}N NMR,[71] OKE,[17] and Raman[5] spectroscopies. Neglecting the different temperatures of the experiments, the data from NMR and OKE are in reasonable agreement. However, the Raman data are systematically lower, whereas the DRS values are significantly higher. Except for Raman, all methods yielded rotational correlation times increasing with urea concentration, as expected from the corresponding rise of solution viscosity (Table S1†).

The methods behind the data of Fig. 8 probe the reorientation of different vectors, namely the dipole vector along the *z*-axis (Fig. 1) in the case of DRS (involving rotation around *x* & *y*); the vector normal to the plane defined by the O, C and N atoms (*i.e.* along *y*-axis, Fig. 1) in the case of OKE (invoking rotation around *x* & *z*);[17] the CN bond in Raman;[5] and the NH bond in the case of NMR[71] (both invoking *x*, *y*, & *z*). Disagreement between the various rotational correlation times, in particular the significantly larger DRS values, thus suggest either anisotropic rotational diffusion of the hydrated urea molecules or their reorientation through large-angle jumps.[72] The linear dependence of $\tau^{(1)}_{DRS,1}$ on viscosity (Fig. 9) suggests rotational diffusion as the mechanism of urea reorientation, see below. Since we may reasonably assume that in this case the experimental rotational correlation times are dominated by the fastest pathway and rotation around the *x* axis is possible both for DRS and OKE, the significantly smaller values for $\tau^{(2)}_{OKE}$ compared to $\tau^{(1)}_{DRS,1}/3$ (Fig. 8) suggest that the OKE signal – as well as NMR and Raman – mainly reflects rotation around the *z* axis. This would be compatible with the hydration-shell structure and the possible urea aggregates discussed by Stumpe and Grubmüller.[36]

For rotational diffusion the extended Stokes-Einstein-Debye equation[73]

$$\tau^{(1)} = \frac{3V_{\text{eff}}\eta}{k_B T} + \tau^0_{\text{rot}} \qquad (8)$$

predicts a linear relation between $\tau^{(1)}_{\text{DRS,1}}$ and solution viscosity, η, with the slope defined by the effective volume of rotation, V_{eff}, of the considered species. The observed intercept, τ^0_{rot} = (11.2 ± 0.2) ps, is commonly interpreted as a free-rotor correlation time,[74] whereas $V_{\text{eff}} = f_\perp C V_m$ with V_m as the intrinsic volume of the molecule and shape factor, $f_\perp$, defined as the ratio of the volume swept out by the rotating particle to the intrinsic volume.[74] The hydrodynamic friction coefficient, C, links macroscopic viscosity to molecular hydrodynamics. Its experimental value is commonly found to be between the theoretical limits for stick, C = 1, and slip boundary conditions, $C = 1 - f_\perp^{-2/3}$, albeit generally closer to the latter.

Fig. 9 illustrates that, irrespective of temperature, all obtained rotational correlation times, $\tau^{(1)}_{\text{DRS, 1}}$, collapse on the same straight line when plotted against η. This finding is a strong hint at rotational diffusion of urea and, in view of Fig. 8, that this motion is anisotropic. Based on OKE spectroscopy and MD simulations Idrissi *et al.*[17, 18] reached the same conclusion.

From the slope of the present data an effective volume of V_{eff} = (11.7 ± 0.2) Å^3 was obtained, which is considerably smaller than the molecular volume from quantum chemical calculations, V_m = 78 ± 11 Å^3. Comparison of V_m and V_{eff} using $f_\perp$ = 1.036 yielded an effective friction coefficient of C = 0.14. This value significantly exceeds the theoretical slip limit of 0.02 and thus indicates strong urea-water interactions, in line with the observed hydration numbers. However, the obtained C and respectively V_{eff} values are not large enough to be compatible with the reorientation of stiff long-lived U·H_2O, U·2H_2O or U·3H_2O complexes. In line with MD simulations[35] and the results of our NCI analysis (see below) it is thus more probable that the common reason for the large friction coefficient, C = 0.14, of urea rotation and the 'missing' Z_t dipoles from the water amplitude, S_b, is the coupled reorientation of solute and hydrating H_2O with a common relaxation time, τ_1, leading to a retardation of the latter by a factor of ~2.2-3.3 compared to the bulk.

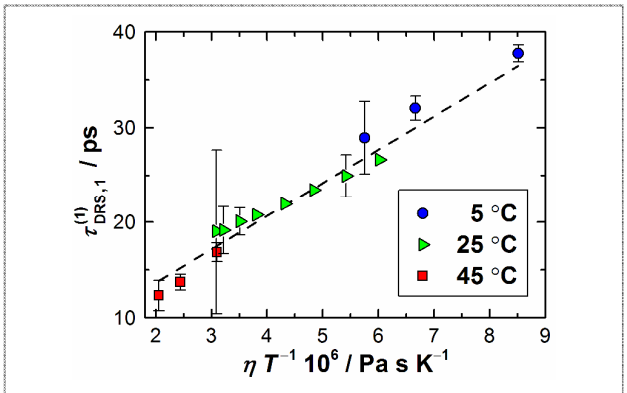

Fig. 9. Rotational correlation time of urea, $\tau^{(1)}_{\text{DRS,1}}$, as a function of η/T. Symbols indicate experimental data; the line represents the fit with eqn (8).

Water reorientation essentially occurs through large-angle jumps,[53] so that analysis of the present τ_2 values with eqn (7) is not appropriate. However, valuable information can be obtained from the temperature dependence of this quantity.

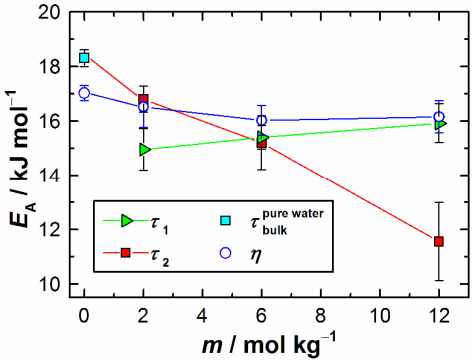

Fig. 10. Arrhenius activation energies, E_A, of the relaxation times of bulk-like water, τ_2, and urea, τ_1, as well as of viscosity, η, for {urea+water} mixtures as a function of solute molality, m.

Accordingly, Fig. 10 compares Arrhenius activation energies, E_A, of viscosity and τ_2 for pure water and for solutions with (2.0, 6.0 and 12.0) mol kg^{-1} urea, determined from the slopes, E_A/k_B, of ln(τ_2) respectively ln(η) plotted against T^{-1}. Additionally, the E_A values for τ_1 are included.

In contrast to Grant *et al,*[10] where $E_A(\tau_1)$ was found to decrease from 35.1 kJ mol^{-1} at 1.0 M to 20.5 kJ mol^{-1} at 9.0 M urea(aq), the present activation energies for urea relaxation are practically independent of concentration, $E_A(\tau_1) \approx$ 15.0 kJ mol^{-1} (Fig. 10) and considerably smaller. Moreover, the present data essentially coincide with $E_A(\eta)$, which explains why all obtained rotational correlation times, $\tau^{(1)}_{\text{DRS,1}}$, collapse on the same straight line when plotted against η / T. The finding of $E_A(\tau_1) \approx E_A(\eta) \approx$ constant is therefore a further stark hint at rotational diffusion as the relaxation mechanism for urea reorientation.

In contrast to the solute, the activation energy for the cooperative water relaxation, $E_A(\tau_2)$, decreases linearly from ~ 18.3 kJ mol^{-1} for pure water to ~ 11.6 kJ mol^{-1} at 12 mol kg^{-1} urea(aq). This suggests a considerable reduction of the average number of H-bonds formed by the 'bulk-like' water molecules.[75] Of course, this is not really surprising for a solution with 12 mol kg^{-1} urea, corresponding to a solute to solvent ratio of 1:4.6, where due to hydration (Fig. 5) on average only ~ 3.5 H_2O per urea molecule contribute to the 'bulk'.

Noncovalent interactions

As shown above, for all studied urea solutions a relaxation of bulk-like water is present, *i.e.* a mode that smoothly evolves in amplitude and relaxation time from the corresponding values of pure water. On the other hand, approximately one H_2O molecule is strongly bound by urea in the most concentrated solution (17.995 mol kg^{-1}), where the solute to solvent ratio is only 1:3. This means that all water molecules are located within the first hydration layer of urea. One can expect that the behavior of water molecules is determined by their local microenvironment, *i.e.*, by the group of molecules it directly interacts with. Urea possesses two hydrophilic moieties, the carbonyl oxygen and the amino hydrogens, capable of H-bonding with water molecules. Thus, a detailed study of urea-water hydrates on the microscopic level is necessary to get deeper insight into the hydration pattern of urea. From this point of view, quantum chemical calculations seem to be the most promising method. Binding energies, however, can only help to assess the relative stability of the various species. In order to estimate the forces within the complex a more sophisticated approach should be used.

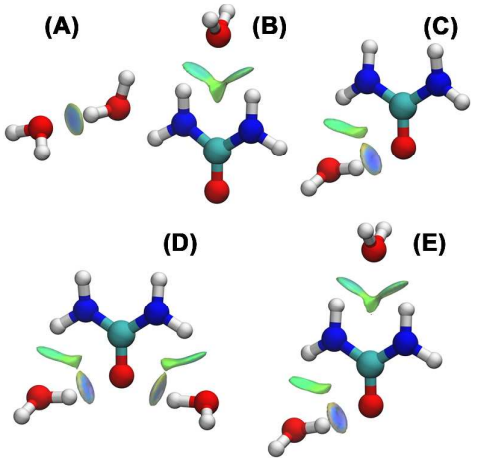

Fig. 11. NCI surfaces for the water dimer (A) and the urea hydrates (B-E) obtained at the B3LYP / 6-311++G(d,p) level of theory in aqueous medium. The reduced-density cut off value is 0.7 a.u., the isosurface is colored according to a blue-green-red scheme over the range -0.04 a.u. < $\mathrm{sign}(\lambda_2)\times\rho$ < 0.04 a.u.

To this end, the recently developed noncovalent interactions (NCIs) analysis,[76, 77] was employed. The NCI index enables studying the domains of the electronic density associated with weak interactions that exhibit both low electron density and a small reduced-density gradient. The latter is defined as

$$s = \frac{1}{2(3\pi)^{1/3}} \frac{|\nabla\rho|}{\rho^{4/3}}, \qquad (9)$$

where ρ is the electron density. By multiplying the electron density by the sign of the second eigenvalue of the density Hessian, λ_2, one can classify strength and nature of the interactions. Negative values of $\mathrm{sign}(\lambda_2)\times\rho$ indicate attractive

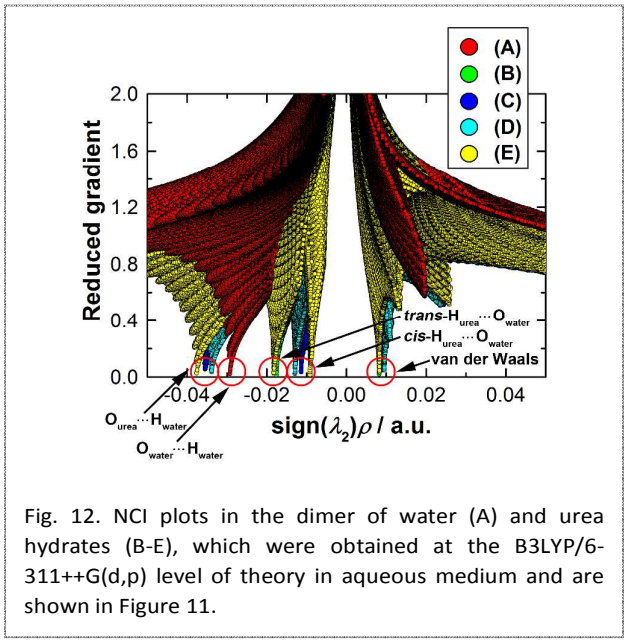

Fig. 12. NCI plots in the dimer of water (A) and urea hydrates (B-E), which were obtained at the B3LYP/6-311++G(d,p) level of theory in aqueous medium and are shown in Figure 11.

interactions (*e.g.* H-bonding); positive values of $\mathrm{sign}(\lambda_2)\times\rho$ point out nonbonding interactions (steric repulsion), whereas values close to zero are indicative of weak van der Waals interactions. In the present case the NCIs were estimated by means of the MultiWFN software.[78]

The NCIs for a water dimer and the urea hydrates B-E of Table 1 are displayed as isosurfaces in Fig. 11. Here, a blue surface indicates a region of strong attraction and green zones indicate weak attractive interaction. Red areas would represent strong repulsion but were not found for the present aggregates. For all hydrates studied localized regions of rather strong noncovalent contacts are found. The most bluish regions, comparable in strength to water-water interactions, correspond to the zones between the urea oxygen atom and water hydrogen (structures C, D and E). Their intensities are almost independent of the number and location of the solvated H_2O molecules. These structures are additionally stabilized by less intense attractive interactions of the *cis*-hydrogen atoms of urea with the water oxygen. On the other hand, interactions of the *trans*-hydrogen atoms of urea with water oxygen (structures B and E) are characterized by somewhat weaker attractions than those between water molecules.

More information on the strength of NCIs is revealed from a graphical representation of the reduced gradient, *s*, as a function of $\mathrm{sign}(\lambda_2)\times\rho$ which is shown in Fig. 12. The characteristic spikes of zero reduced gradient around $\mathrm{sign}(\lambda_2)\times\rho$ = 0.01 correspond to weak van der Waals interactions within the urea hydrates. Strongly repulsive interactions, corresponding to $s \approx 0$ at $\mathrm{sign}(\lambda_2)\times\rho > 0.02$ were not observed. On the other hand, the narrow sharp minima of *s* at negative abscissa values are typical for strong attractive noncovalent interactions. Based on the location of the corresponding isosurfaces (Fig. 11), these were assigned to H-bonds between the interaction sites indicated in Fig. 12. Their strengths are in the sequence O_{urea}-H_{water} > O_{water}-H_{water} >

trans-H_{urea}-O_{water} > *cis*-H_{urea}-O_{water}, in line with H-bond lifetimes from the MD simulation of Kokubo *et al.*[35] which also decrease in the order O_{urea}-H_{water} > O_{water}-H_{water} > H_{urea}-O_{water}.

For structures B and E both H-bonds involving the *trans*-hydrogen atoms of urea and the water molecule bridging them are weaker than the bond in the water-water dimer. Water molecules located near the carbonyl oxygen also form two H-bonds with urea (Fig. 11, structures C, D & E). Now one of them is between the carbonyl oxygen and one of the water hydrogens, whereas the second involves the *cis*-hydrogen of urea and water oxygen. According to Fig. 12 the first is definitely stronger than a H_2O-H_2O bond whereas the second is weaker. Two solvent molecules can be bound in such a rather rigid configuration (Fig. 11, structure D) and most likely it is these two H_2O which are strongly impeded in their reorientation by urea and thus detected as Z_t by DRS.

Conclusions

We studied the dielectric response of {urea+water} mixtures over a wide concentration range and at different temperatures. In contrast to earlier DRS studies, the present investigation results in an unambiguous separation of the urea and water relaxation modes in the dielectric spectra. The more accurate fit parameters, in particular solute and water relaxation times and amplitudes, allowed deeper insight into the hydration of urea.

In agreement with previous studies, we find a hydration number of 2 for urea at infinite dilution. This value decreases with increasing solute concentration to ~ 0.8 H_2O molecules per urea at 10 M. The effective dipole moment of the solute is significantly higher than that of a urea molecule, indicating pronounced parallel solute-solvent correlations in solutions through the formation of rather stable urea-water complexes. In line with the obtained effective hydration numbers, Z_t, the weak decrease of the effective solute dipole moment with increasing urea concentration suggests dehydration due to solvation-shell overlap.

Urea reorientation can be described as anisotropic rotational diffusion governed by solution viscosity. This includes the Z_t strongly bound water molecules which move together with the solute dipole. The remaining bulk-like water exhibits only a slight increase of its relaxation time compared to pure H_2O. This increase does not scale with viscosity but is accompanied by a strong decrease of the Arrhenius activation energy, $E_A(\tau_2)$, indicating a significant decrease of the number of hydrogen bonds formed by the involved water molecules.

Quantum chemical calculations of the urea hydrates show that the energetically most stable complexes are characterized by double H-bonding of water with urea occurring either via both *trans*-hydrogens or the carbonyl oxygen and the *cis*-hydrogens of a urea. In order to estimate the strength and location of these H-bonds, a noncovalent-interactions (NCIs) analysis was applied to the urea-water complexes and water dimer. It was shown that the strengths of these interactions are in the sequence O_{urea}-H_{water} > O_{water}-H_{water} > *trans*-H_{urea}-O_{water} > *cis*-H_{urea}-O_{water}. From this data it can be inferred that the reorientational dynamics of those H_2O molecules doubly H-bonded with urea through the carbonyl oxygen and the *cis*-hydrogens is substantially slowed down compared to the dynamics of water in bulk. As a consequence, these water molecules most probably represent the water fraction strongly bound to urea.

Acknowledgements

V. A. acknowledges support from the Russian Government Program for Competitive Growth of Kazan Federal University and thanks the Deutscher Akademischer Austausch-dienst (DAAD) for a grant enabling her experiments in Regensburg. We would also like to thank a reviewer for drawing our attention Ref. 36.

Notes and references

1 J. Grdadolnik and Y. Maréchal, *J. Mol. Struct.*, 2002, **615**, 177-189.
2 Y. M. Jung, *Bull. Kor. Chem. Soc.*, 2003, **24**, 1243-1244.
3 Y. L. A. Rezus and H. J. Bakker, *Proc. Nat. Acad. Sci.*, 2006, **103**, 18417-18420.
4 Y. Mizutani, K. Kamogawa and K. Nakanishi, *J. Phys. Chem.*, 1989, **93**, 5650-5654.
5 X. Hoccart and G. Turrell, *J. Chem. Phys.*, 1993, **99**, 8498-8503.
6 K. Mazur, I. A. Heisler and S. R. Meech, *J. Phys. Chem. B*, 2011, **115**, 2563-2573.
7 S. Subramanian, T. S. Sarma, D. Balasubramanian and J. C. Ahluwalia, *J. Phys. Chem.*, 1971, **75**, 815-820.
8 A. Shimizu, K. Fumino, K. Yukiyasu and Y. Taniguchi, *J. Mol. Liq.*, 2000, **85**, 269-278.
9 L. Costantino, G. D'Errico, O. Ortona and V. Vitagliano, *J. Mol. Liq.*, 2000, **84**, 179-191.
10 E. H. Grant, S. E. Keefe and R. Shack, *Adv. Mol. Relax. Pr.*, 1972, **4**, 217-228.
11 R. Pottel, D. Adolph and U. Kaatze, *Ber. Bunseng. Phys. Chem.*, 1975, **79**, 278-285.
12 U. Kaatze, H. Gerke and R. Pottel, *J. Phys. Chem.*, 1986, **90**, 5464-5469.
13 J. B. Bateman, C. Gabriel, G. F. Evans and E. H. Grant, *J. Chem. Soc., Faraday Trans.*, 1990, **86**, 321-328.
14 A. Saito, O. Miyawaki and K. Nakamura, *Biosci., Biotechnol., Biochem.*, 1997, **61**, 1831-1835.
15 Y. Hayashi, Y. Katsumoto, S. Omori, N. Kishii and A. Yasuda, *J. Phys. Chem. B*, 2007, **111**, 1076-1080.
16 Y. Hayashi, Y. Katsumoto, I. Oshige, S. Omori and A. Yasuda, *J. Phys. Chem. B*, 2007, **111**, 11858-11863.
17 A. Idrissi, P. Bartolini, M. Ricci and R. Righini, *J. Chem. Phys.*, 2001, **114**, 6774-6780.
18 A. Idrissi, P. Bartolini, M. Ricci and R. Righini, *Phys. Chem. Chem. Phys.*, 2003, **5**, 4666-4671.
19 S. Funkner, M. Havenith and G. Schwaab, *J. Phys. Chem. B*, 2012, **116**, 13374-13380.
20 N. Samanta, D. Das Mahanta and R. Kumar Mitra, *Chem. Asian J.*, 2014, **9**, 3457-3463.
21 J. Turner, J. L. Finney and A. K. Soper, *Z. Naturforsch. A*, 1991, **46**, 73-83.

22 Y. Kameda, H. Naganuma, K. Mochiduki, M. Imano, T. Usuki and O. Uemura, *Bull. Chem. Soc. Jpn.*, 2002, **75**, 2579-2585.
23 Y. Kameda, M. Sasaki, S. Hino, Y. Amo and T. Usuki, *Bull. Chem. Soc. Jpn.*, 2006, **79**, 1367-1371.
24 Y. Kameda, A. Maki, Y. Amo and T. Usuki, *Bull. Chem. Soc. Jpn.*, 2010, **83**, 131-144.
25 R. Adams, H. H. M. Balyuzi and R. E. Burge, *J. Appl. Crystallogr.*, 1977, **10**, 256-261.
26 P. O. Åstrand, A. Wallqvist, G. Karlström and P. Linse, *J. Chem. Phys.*, 1991, **95**, 8419-8429.
27 J. Hernández-Cobos, I. Ortega-Blake, M. Bonilla-Marín and M. Moreno-Bello, *J. Chem. Phys.*, 1993, **99**, 9122-9134.
28 A. Tovchigrechko, M. Rodnikova and J. Barthel, *J. Mol. Liq.*, 1999, **79**, 187-201.
29 B. Kallies, *Phys. Chem. Chem. Phys.*, 2002, **4**, 86-95.
30 A. K. Soper, E. W. Castner Jr and A. Luzar, *Biophys. Chem.*, 2003, **105**, 649-666.
31 T. Ishida, P. J. Rossky and E. W. Castner, *J. Phys. Chem. B*, 2004, **108**, 17583-17590.
32 A. Idrissi, E. Cinar, S. Longelin and P. Damay, *J. Mol. Liq.*, 2004, **110**, 201-208.
33 A. Idrissi, P. Damay and M. Kiselev, *Chem. Phys.*, 2007, **332**, 139-143.
34 A. Idrissi, M. Gerard, P. Damay, M. Kiselev, Y. Puhovsky, E. Cinar, P. Lagant and G. Vergoten, *J. Phys. Chem. B*, 2010, **114**, 4731-4738.
35 H. Kokubo and B. M. Pettitt, *J. Phys. Chem. B*, 2007, **111**, 5233-5242.
36 M. C. Stumpe and H. Grubmüller, *J. Phys. Chem. B*, 2007, **111**, 6220-6228.
37 A. K. H. Weiss and T. S. Hofer, *Mol. BioSyst.*, 2013, **9**, 1864-1876.
38 J. K. Carr, L. E. Buchanan, J. R. Schmidt, M. T. Zanni and J. L. Skinner, *J. Phys. Chem. B*, 2013, **117**, 13291-13300.
39 S. Weerasinghe and P. E. Smith, *J. Chem. Phys.*, 2003, **118**, 5901-5910.
40 S. Weerasinghe and P. E. Smith, *J. Phys. Chem. B*, 2003, **107**, 3891-3898.
41 A. Idrissi, F. Sokolić and A. Perera, *J. Chem. Phys.*, 2000, **112**, 9479-9488.
42 C. Lee, E. A. Stahlberg and G. Fitzgerald, *J. Phys. Chem.*, 1995, **99**, 17737-17741.
43 F. Ramondo, L. Bencivenni, R. Caminiti, A. Pieretti and L. Gontrani, *Phys. Chem. Chem. Phys.*, 2007, **9**, 2206-2215.
44 F. Kremer and A. Schönhals, eds., *Broadband Dielectric Spectroscopy*, Springer, Berlin, 2003.
45 R. Buchner and G. Hefter, *Phys. Chem. Chem. Phys.*, 2009, **11**, 8984-8999.
46 T. Sonnleitner, D. A. Turton, S. Waselikowski, J. Hunger, A. Stoppa, M. Walther, K. Wynne and R. Buchner, *J. Mol. Liq.*, 2014, **192**, 19-25.
47 S. Schrödle, G. Hefter, W. Kunz and R. Buchner, *Langmuir*, 2006, **22**, 924-932.
48 P. R. Bevington and D. K. Robinson, *Data reduction and error analysis for the physical sciences*, McGraw-Hill, New York, 2003.
49 J. Barthel, R. Buchner, P. N. Eberspächer, M. Münsterer, J. Stauber and B. Wurm, *J. Mol. Liq.*, 1998, **78**, 83-109.
50 A. Y. Zasetsky and R. Buchner, *J. Phys.: Condens. Matter*, 2011, **23**, 025903.
51 T. Fukasawa, T. Sato, J. Watanabe, Y. Hama, W. Kunz and R. Buchner, *Phys. Rev. Lett.*, 2005, **95**, 197802.
52 J. Hunger, N. Ottosson, K. Mazur, M. Bonn and H. J. Bakker, *Phys. Chem. Chem. Phys.*, 2015, **17**, 298-306.
53 D. Laage, G. Stirnemann, F. Sterpone, R. Rey and J. T. Hynes, *Annu. Rev. Phys. Chem.*, 2011, **62**, 395-416.
54 Costantino *et al.*[9] assume viscosity to be independent of urea concentration. Correction of their diffusion data with the present η values (Table S1†) yields an even higher NMR hydration number of 10.5 ± 0.4.
55 A. Panuszko, P. Bruździak, J. Zielkiewicz, D. Wyrzykowski and J. Stangret, *J. Phys. Chem. B*, 2009, **113**, 14797-14809.
56 F. Meersman, D. Bowron, A. K. Soper and M. H. J. Koch, *Phys. Chem. Chem. Phys.*, 2011, **13**, 13765-13771.
57 V. N. Afanas'ev, *J. Solution Chem.*, 2012, **41**, 1447-1461.
58 J. Krakowiak and J. Wawer, *J. Chem. Thermodyn.*, 2014, **79**, 109-117.
59 J. Barthel, H. Hetzenauer and R. Buchner, *Ber. Bunseng. Phys. Chem.*, 1992, **96**, 1424-1432.
60 J. Hunger, K.-J. Tielrooij, R. Buchner, M. Bonn and H. J. Bakker, *J. Phys. Chem. B*, 2012, **116**, 4783-4795.
61 H. M. A. Rahman, G. Hefter and R. Buchner, *J. Phys. Chem. B*, 2012, **116**, 314-323.
62 A. Eiberweiser, A. Nazet, G. Hefter and R. Buchner, *J. Phys. Chem. B*, 2015, **119**, 5270-5281.
63 R. Buchner, C. Holzl, J. Stauber and J. Barthel, *Phys. Chem. Chem. Phys.*, 2002, **4**, 2169-2179.
64 H. M. A. Rahman, G. Hefter and R. Buchner, *J. Phys. Chem. B*, 2013, **117**, 2142-2152.
65 K.-J. Tielrooij, J. Hunger, R. Buchner, M. Bonn and H. J. Bakker, *J. Am. Chem. Soc.*, 2010, **132**, 15671-15678.
66 R. D. Brown, P. D. Godfrey and J. Storey, *J. Mol. Spectrosc.*, 1975, **58**, 445-450.
67 M. J. Frisch, G. W. Trucks, H. B. Schlegel, G. E. Scuseria, M. A. Robb, J. R. Cheeseman, J. A. Montgomery, Jr., T. Vreven, K. N. Kudin, J. C. Burant, J. M. Millam, S. S. Iyengar, J. Tomasi, V. Barone, B. Mennucci, M. Cossi, G. Scalmani, N. Rega, G. A. Petersson, H. Nakatsuji, M. Hada, M. Ehara, K. Toyota, R. Fukuda, J. Hasegawa, M. Ishida, T. Nakajima, Y. Honda, O. Kitao, H. Nakai, M. Klene, X. Li, J. E. Knox, H. P. Hratchian, J. B. Cross, C. Adamo, J. Jaramillo, R. Gomperts, R. E. Stratmann, O. Yazyev, A. J. Austin, R. Cammi, C. Pomelli, J. W. Ochterski, P. Y. Ayala, K. Morokuma, G. A. Voth, P. Salvador, J. J. Dannenberg, V. G. Zakrzewski, S. Dapprich, A. D. Daniels, M. C. Strain, O. Farkas, D. K. Malick, A. D. Rabuck, K. Raghavachari, J. B. Foresman, J. V. Ortiz, Q. Cui, A. G. Baboul, S. Clifford, J. Cioslowski, B. B. Stefanov, G. Liu, A. Liashenko, P. Piskorz, I. Komaromi, R. L. Martin, D. J. Fox, T. Keith, M. A. Al-Laham, C. Y. Peng, A. Nanayakkara, M. Challacombe, P. M. W. Gill, B. Johnson, W. Chen, M. W. Wong, C. Gonzalez and J. A. Pople, *Journal*, 2003.
68 J. B. Foresman, T. A. Keith, K. B. Wiberg, J. Snoonian and M. J. Frisch, *J. Phys. Chem.*, 1996, **100**, 16098-16104.
69 J. G. Powles, *J. Chem. Phys.*, 1953, **21**, 633-637.
70 S. H. Glarum, *J. Chem. Phys.*, 1960, **33**, 639-643.
71 E. G. Finer, F. Franks and M. J. Tait, *J. Am. Chem. Soc.*, 1972, **94**, 4424-4429.
72 J. Hunger, A. Stoppa, S. Schrödle, G. Hefter and R. Buchner, *ChemPhysChem*, 2009, **10**, 723-733.
73 J. L. Dote, D. Kivelson and R. N. Schwartz, *J. Phys. Chem.*, 1981, **85**, 2169-2180.
74 J. L. Dote and D. Kivelson, *J. Phys. Chem.*, 1983, **87**, 3889-3893.
75 R. Buchner, J. Barthel and J. Stauber, *Chem. Phys. Lett.*, 1999, **306**, 57-63.

76 J. Contreras-García, E. R. Johnson, S. Keinan, R. Chaudret, J.-P. Piquemal, D. N. Beratan and W. Yang, *J. Chem. Theory Comput.*, 2011, **7**, 625-632.
77 E. R. Johnson, S. Keinan, P. Mori-Sánchez, J. Contreras-García, A. J. Cohen and W. Yang, *J. Am. Chem. Soc.*, 2010, **132**, 6498-6506.
78 T. Lu and F. Chen, *J. Comput. Chem.*, 2012, **33**, 580-592.